the same flock. Even individual fish with their multiple fins recycle the wake of their own upstream propellers for increased power and control. An improved understanding of these natural mechanisms should help engineers to design better foil propulsors. The next step will be to seek more examples of phase-locked swimming and flight movements in nature to ascertain how widely vortex recycling is exploited during swimming and flight.

References

1. J. C. Liao, D. N. Beal, G. V. Lauder, M. S. Triantafyllou, *Science* **302**, 1566 (2003).
2. J. Zhang *et al.*, *Nature* **408**, 835 (2000).
3. L. Prandtl, *Essentials of Fluid Mechanics* (Hafner, New York, 1952).
4. U. K. Müller *et al.*, *Integr. Comp. Biol.* **42**, 981 (2002).
5. J. M. Birch, M. H. Dickinson, *J. Exp. Biol.* **206**, 2257 (2003).
6. M. J. McHenry *et al.*, *J. Exp. Biol.* **198**, 2293 (1995).
7. J. C. Liao *et al.*, *J. Exp. Biol.* **206**, 1059 (2003).
8. G. R. Spedding *et al.*, *J. Exp. Biol.* **206**, 2313 (2003).

ATMOSPHERIC SCIENCE

Nitrogen and Climate Change

Bruce A. Hungate, Jeffrey S. Dukes, M. Rebecca Shaw, Yiqi Luo, Christopher B. Field

Human activities, particularly burning fossil fuel, have increased atmospheric carbon dioxide (CO_2) concentrations. Because CO_2 traps heat, continued emissions are expected to change global climate. The extent of this change will depend not only on the rate of emissions, but also on carbon uptake by the oceans and the land.

According to some models, land ecosystems can sequester carbon fast enough to help to counteract CO_2 emissions. Models featured in the Third Assessment Report of the Intergovernmental Panel on Climate Change (IPCC) suggest that increasing atmospheric CO_2 alone could cause 350 to 890 Pg of carbon (1 Pg = 10^{15} g) to accumulate in the terrestrial biosphere by 2100. These amounts are equivalent to 22 to 57% of expected anthropogenic CO_2 emissions in an intermediate emissions scenario (*1*, *2*). The models suggest that atmospheric CO_2 and climate change together could cause 260 to 530 Pg of carbon to accumulate, or 16 to 34% of emissions (*1*, *2*).

These models probably exaggerate the terrestrial biosphere's potential to slow atmospheric CO_2 rise. Ecosystem carbon accumulation may be constrained by nutrients, particularly nitrogen (*3*, *4*), through mechanisms that are not well developed in or absent from the models.

How much nitrogen do the model projections require? The models distribute the future terrestrial carbon sink roughly equally between trees and soils. With no change in the carbon:nitrogen (C:N) ratios of trees (200) and soils (15), the CO_2-only projections require 7.7 to 37.5 Pg of nitrogen; the CO_2-climate projections require 2.3 to 16.9 Pg of nitrogen (see the figure) (*5*).

Can increasing ecosystem C:N ratios reduce the nitrogen required? Tree C:N increases with atmospheric CO_2 concentration (*6*, *7*). But even allowing all the simulated increase in tree carbon to occur as wood (C:N = 500) only slightly reduces the amount of additional nitrogen required (see the figure). Soil C:N could also increase with rising atmospheric CO_2 concentration, allowing soil carbon accumulation without additional nitrogen. This mechanism could allow some nitrogen transfer from soil to trees (*6*, *7*), lowering the nitrogen demand associated with increased tree carbon. However, experimental studies show that when CO_2 enrichment increases soil C:N, decomposing microorganisms require more nitrogen. This effect can reduce nitrogen mineralization, the main source of nitrogen for plants (*8*, *9*). It is thus unlikely that increases in soil C:N could yield large increases in ecosystem carbon stocks.

With little contribution from increasing C:N, the carbon-uptake projections (*1*, *2*) almost certainly require nitrogen accumulation. Nitrogen enters the terrestrial biosphere through atmospheric deposition and biological fixation, and is mainly lost through leaching and gaseous fluxes. We have estimated high and low nitrogen fluxes for each of these mechanisms (*10*).

To estimate future anthropogenic nitrogen deposition based on population-growth projections (*11*), we assume that per capita nitrogen deposition remains constant (low) or increases linearly to that of North America today (high) (*12*). We assume that 5% (low) to 10% (high) of that deposited nitrogen supports increased carbon storage (*9*). We estimate biological nitrogen fixation (*12*) to increase linearly by 10% (low) or 45% (high) with CO_2 doubling (*9*). We further assume that nitrogen leaching losses are currently 36 Tg of nitrogen per year (*13*), and that nitrogen leaching would decline linearly with CO_2 doubling by 0 (low) to 20% (high) (*9*).

Combining our high estimates, 6.1 Pg of nitrogen could accumulate by 2100 (see the figure). This amount is less than is required by all CO_2-only simulations and by four of the six CO_2-climate simulations (*1*, *2*) (see the figure). Our low estimates of nitrogen accumulation yield only 1.2 Pg of nitrogen, insufficient for all simulations.

We have focused on nitrogen, but the situation may be worse for other nutrients, such as potassium and phosphorus, which are less subject to human or biological control than is nitrogen fixation. Models that incorporate nutrient cycling predict much less CO_2 carbon uptake than models lacking these feedbacks (*14*). The next IPCC assessment must include models taking into account these feedbacks.

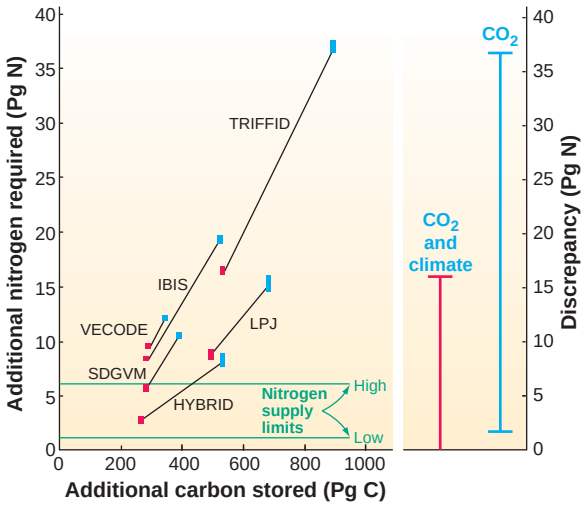

Supply and demand. (**Left**) Nitrogen required to support terrestrial carbon uptake (*1*), compared to likely limits of nitrogen supply (green). For each model (*2*), values are shown for CO_2-only (blue) and CO_2-climate (red) projections. The upper nitrogen requirement assumes a fixed tree C:N of 200; the lower value assumes that all new tree carbon is allocated to wood. (**Right**) Discrepancy between nitrogen required for projected carbon uptake and likely nitrogen availability for CO_2-only (blue) and CO_2-and-climate-change (red) scenarios. Upper value: maximum calculated nitrogen required minus low nitrogen supply limit. Lower value: minimum nitrogen required minus high nitrogen supply limit.

B. A. Hungate is in the Department of Biological Sciences and the Merriam-Powell Center for Environmental Research, Northern Arizona University, Flagstaff, AZ 86011, USA. E-mail: bruce.hungate@nau.edu J. S. Dukes, M. R. Shaw, and C. B. Field are in the Department of Global Ecology, Carnegie Institution of Washington, Stanford, CA 94305, USA. Y. Luo is in the Department of Botany and Microbiology, University of Oklahoma, Norman, OK 73019, USA.

References and Notes

1. J. T. Houghton *et al.*, Eds., *Climate Change 2001: The Scientific Basis* (Cambridge Univ. Press, Cambridge, 2001).
2. W. Cramer *et al.*, *Global Change Biol.* **7**, 357 (2001).
3. K. J. Nadelhoffer *et al.*, *Nature* **398**, 145 (1999).
4. A. R. Townsend *et al.*, *Ecol. Appl.* **6**, 806 (1996).
5. Of the models featured in the IPCC assessment, only the two with the lowest nitrogen requirements include nitrogen cycling (*1*, *2*).
6. B. A. Hungate, in *Carbon Dioxide and Environmental Stress*, Y. Luo, H. Mooney, Eds. (Academic Press, San Diego, CA, 1999), pp. 265–285.
7. E. B. Rastetter *et al.*, *Water Air Soil Poll.* **64**, 327 (1992).
8. R. A. Gill *et al.*, *Nature* **417**, 279 (2002).
9. Methods are available as supporting material on *Science* Online.
10. We did not include CO_2 or climate change effects on nitrogen gas losses, because experimental results are ambiguous (*5*).
11. W. Lutz *et al.*, *Nature* **412**, 543 (2001).
12. J. N. Galloway, E. B. Cowling, *Ambio* **31**, 64 (2002).
13. W. H. Schlesinger, *Biogeochemistry: An Analysis of Global Change* (Academic Press, San Diego, CA, 1997).
14. D. W. Kicklighter *et al.*, *Tellus* **51B**, 343 (1999).

15. Supported by the NSF, U.S. Department of Energy, and the National Center for Ecological Analysis and Synthesis. We thank G. Ågren, W. Currie, D. Johnson, D. Kicklighter, G. Koch, A. Langley, W. Lucht, R. D. McGuire, McMurtrie, P. Megonigal, D. Pataki, L. Pitelka, and B. Smith for helpful discussions and G. Merchant for help with the data analysis.

Supporting Online Material

www.sciencemag.org/cgi/content/full/302/5650/1512/DC1
Methods
References

STRUCTURAL BIOLOGY

Nuclear Trafficking

Murray Stewart

The trafficking of proteins into and out of the nucleus is a striking example of a crucial cellular process that is mediated by a series of finely choreographed protein-protein interactions (*1*). The importin-β family of nuclear transport proteins interacts with an extraordinarily diverse series of cargo proteins, posing exquisite problems of molecular recognition and control. Crystal structures of importin-β:cargo complexes (*2*–*10*) provide powerful insights into the molecular basis of this recognition. On page 1571, Lee *et al.* (*10*) describe how importin-β combines specific surface recognition sites with conformational flexibility to facilitate recognition of many different binding partners. They highlight the crystal structure of importin-β bound to a transcription factor SREBP-2 (sterol regulatory element–binding protein 2), which regulates the expression of genes controlling cholesterol metabolism.

Macromolecules move back and forth between the nucleus and cytoplasm through cylindrical structures called nuclear pore complexes (NPCs) (*11*). The nuclear import and export of large macromolecules is an energy-dependent process mediated by soluble transport factors that bind to cargo proteins in one cellular compartment, translocate them through NPCs, and then release them in the other compartment before being recycled through the NPCs to participate in another round of transport (*1*). Many transport factors belong to the importin-β superfamily, and, frequently, their interactions with both cargo proteins and NPC proteins (nucleoporins) are orchestrated by Ran guanosine triphosphatase (Ran GTPase). Because of the spatial distribution of its GAP and GEF proteins, cytoplasmic Ran is primarily in the GDP-bound state, whereas nuclear Ran is primarily in the GTP-bound state (*1*).

The author is at the MRC Laboratory of Molecular Biology, Cambridge CB2 2QH, UK. E-mail: ms@mrc-lmb.cam.ac.uk

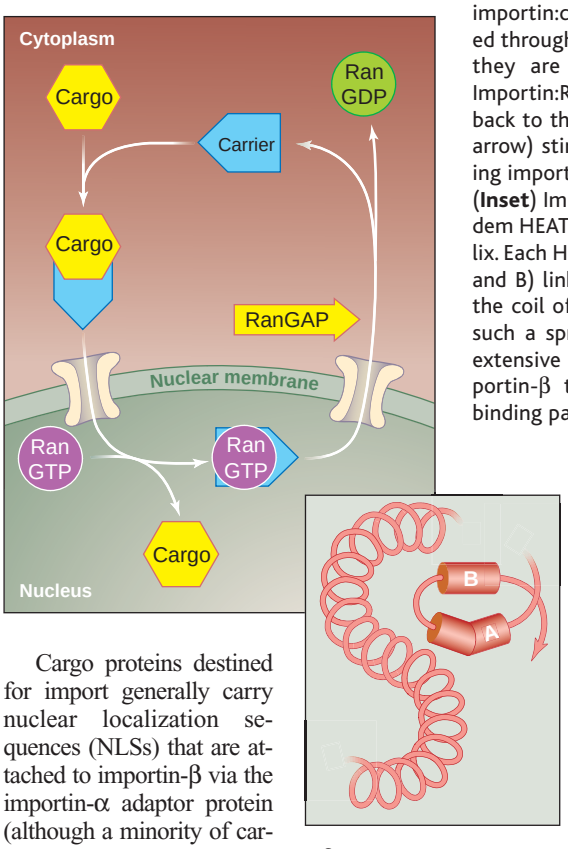

Regulating traffic flow. Transport of cargo proteins (yellow) between the cytoplasm and nucleus is mediated by carrier molecules such as importin-β (blue). During nuclear import, the carrier binds to a cargo protein in the cytoplasm, often via the importin-α adaptor. The importin:cargo complexes are then transported through nuclear pores to the nucleus where they are dissociated by RanGTP (purple). Importin:RanGTP complexes are then recycled back to the cytoplasm where RanGAP (yellow arrow) stimulates the hydrolysis of GTP, freeing importin-β for another round of transport. (**Inset**) Importin-β is constructed from 19 tandem HEAT repeats that coil to form a superhelix. Each HEAT repeat contains two α helices (A and B) linked by flexible loops and resembles the coil of a spring. The flexibility inherent in such a springlike molecule, together with an extensive interaction interface, enables importin-β to recognize a broad spectrum of binding partners.

Cargo proteins destined for import generally carry nuclear localization sequences (NLSs) that are attached to importin-β via the importin-α adaptor protein (although a minority of cargo proteins bind to importin-β directly). Importin-α binds to importin-β through its amino-terminal IBB (importin-β binding) domain. The passage of importin-β:cargo complexes through NPCs is mediated by transient interactions with nucleoporins that have characteristic FG sequence repeats (*7*, *8*). Finally, nuclear RanGTP binds to importin-β, inducing release of its cargo and facilitating the recycling of importin back to the cytoplasm. In addition to its central role in nuclear import, importin-β also appears to be involved at several stages in cell division (*12*, *13*). Because it binds to such a remarkably wide range of partners, importin-β must exhibit astonishing versatility in molecular recognition.

Importin-β has a modular structure based on 19 tandem HEAT repeats arranged to form a superhelix (*3*, *5*, *6*, *10*). Each HEAT repeat represents a structural motif formed from two α helices joined by a loop (see the figure). In two HEAT repeats (7 and 17), one of the helices is unusually long and so generates a protrusion from the molecule in this region. The HEAT array generates an extensive surface that enables importin-β to act as a molecular scaffold. One helix of each HEAT repeat faces the inner, concave surface, and the other forms the outer, convex surface. The array of linked helices produces a springlike structure with intrinsic flexibility. Some members of the importin-β family show considerable conformational variation between different functional states (*14*). Importin-β, for example, has an S-shaped conformation in the absence of bound cargo, but adopts a more compact helicoidal shape when bound to the IBB domain of importin-α or to RanGTP. Binding of RanGTP to importin-β probably involves a less dramatic overall conformational change. However, this change is sufficient to alter the affinity of im-

CREDIT: ADAPTED BY PRESTON HUEY/*SCIENCE*